

IRIS 2010/2012 Rigid Missile Perforation of Reinforced Concrete Slab with new LS-DYNA features

Eric Piskula¹

¹ANSYS Inc France

1 Introduction

Modeling the nonlinear behavior of concrete and reinforced concrete (RC) structures under high-intensity loads is a complex challenge. These loads can cause material compaction, fragmentation, and cracking, making accurate simulations essential for the design of civil structures, especially when experimental data is unavailable. This study presents a methodology to evaluate both global and local strength of RC components using the LS-DYNA solver. In December 2008, the Committee on the Safety of Nuclear Installations approved a proposal from the Working Group on Integrity and Ageing of Components and Structures to launch the **IRIS_2010** benchmarking study (Improving Robustness Assessment of Structures Impacted by MissileS)[1]. The goal was to compare different computational tools, modeling techniques, and results to analyze the structural response of nuclear power plant (NPP) structures to missile impacts, improving accuracy and fostering international collaboration without destructive testing. The IRIS_2010 study focused on RC elements, such as walls and slabs, subjected to missile impacts at medium velocities (100–200 m/s). Failure mechanisms like bending and punching were analyzed. It was considered more interesting (and exciting) to propose blind simulations in 2010 to test modeling capabilities. Initial simulation results were unsatisfactory [2], prompting a second phase in 2012 [3] with additional experimental data to improve accuracy and bring results closer to real-world observations. This study revisits these simulations using the same data from 2010 and 2012 but with enhanced features of LS-DYNA as of 2025. The goal is to evaluate improvements in accuracy due to technological advancements. To reduce the number of simulations, this study focuses solely on the perforation of a reinforced concrete slab by a rigid missile, a critical failure mode in structural safety analysis, providing a test case for modern modeling technics.

2 VTT Punching Test

Two tests involving the impact of a missile into a steel reinforced concrete panel were conducted at the VTT Technical Research Center of Finland in 2010 for the IRIS round-robin study, one which is referred to as the VTT Punching test with a Rigid Missile projectile intended to generate an impact of hard type.

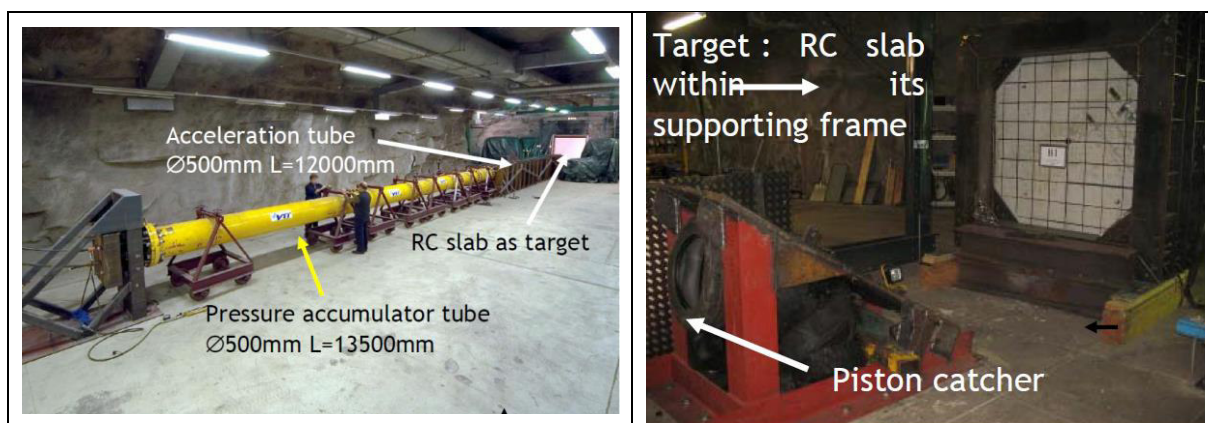


Fig.1: VTT Punch Test Facility

The VTT Punching test made use of a relatively rigid 47.4 kg light weight concrete filled steel pipe missile with a 0.168 m outer diameter and total length of 0.64 m (not including a smaller diameter aluminum pipe attached to the trailing end of the missile used to determine its velocity during the impact). The pipe's wall thickness was constant along its length at 10 mm. The pipe was capped with a thick steel dome on its leading end (Figure 2).

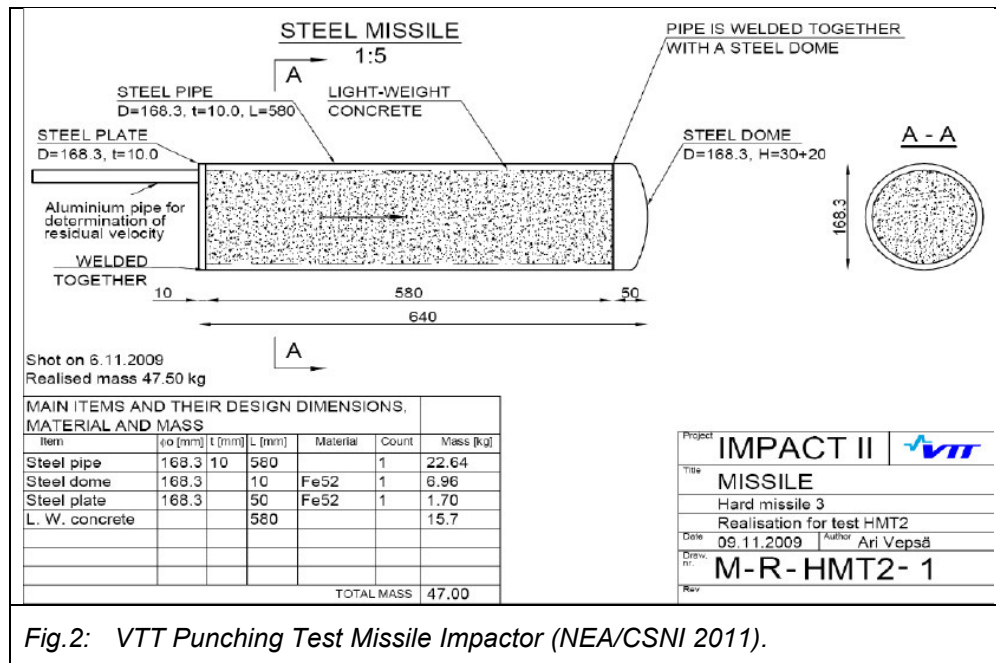


Fig.2: VTT Punching Test Missile Impactor (NEA/CSNI 2011).

The target was a 2.1 m square (length and width), 0.25 m thick steel-reinforced concrete panel simply supported along its four edges as illustrated in Figure 3. The unsupported span, both in length and width directions, was 2.0 m. Bending reinforcement consisted of 10 mm diameter A500HW steel bars with a density of 8.7 cm²/m running in both the length and width directions on each face (front and back) of the panel. No shear (through thickness) reinforcement was used.

The missile impact velocity was 135.9 m/s. The response of the target was dominated by a shear punching failure in which the missile perforated the target and exited the back side with a non-zero residual average velocity of 38.48 m/s (Figure 4).

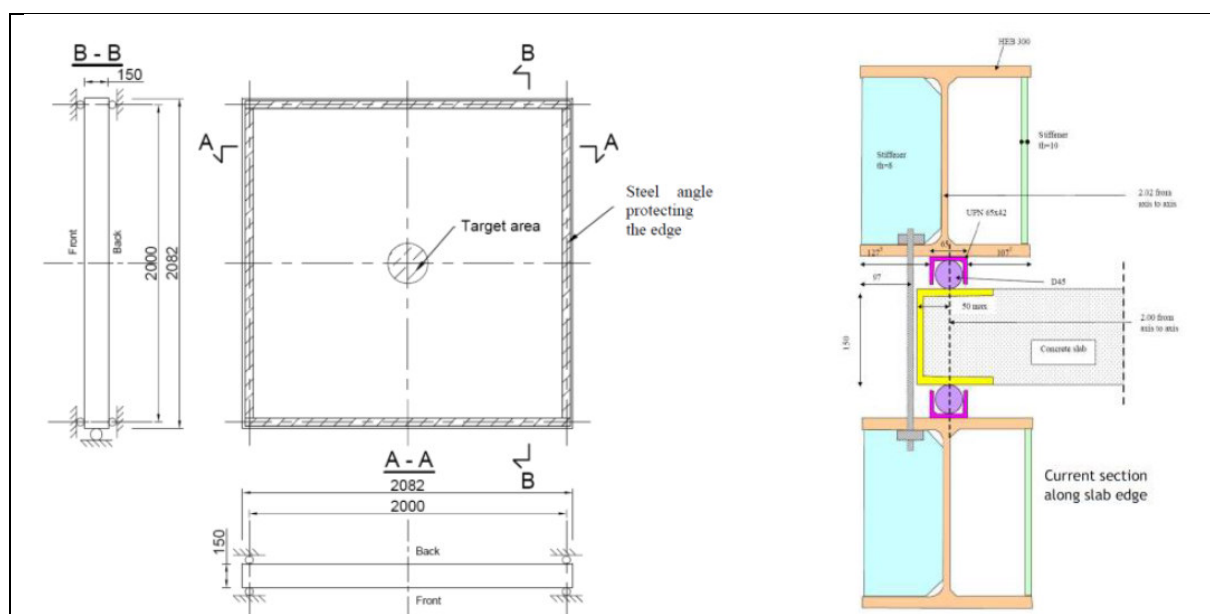


Fig.3: VTT Punching Test Target Support Conditions (NEA/CSNI 2011).

During the test, the missile perforated the wall and caused a layer of concrete to come loose at the back surface of the wall (scabbing). This perforation happened in each punching behavior test.

Table 1: Missile Velocities measured with 3 identical tests performed

Velocity (m/s)	Slab P1	Slab P2	Slab P3
Initial	136	135	136
Residual	33.8	45.3	35.8

Figure 5 shows how large the damaged areas of walls were in the punching tests. The drawings show the scabbed area at the backside of the wall (a) and the spalling area on the front side of the wall (b). The circular shapes near the center represent the holes made in the walls by the missile.

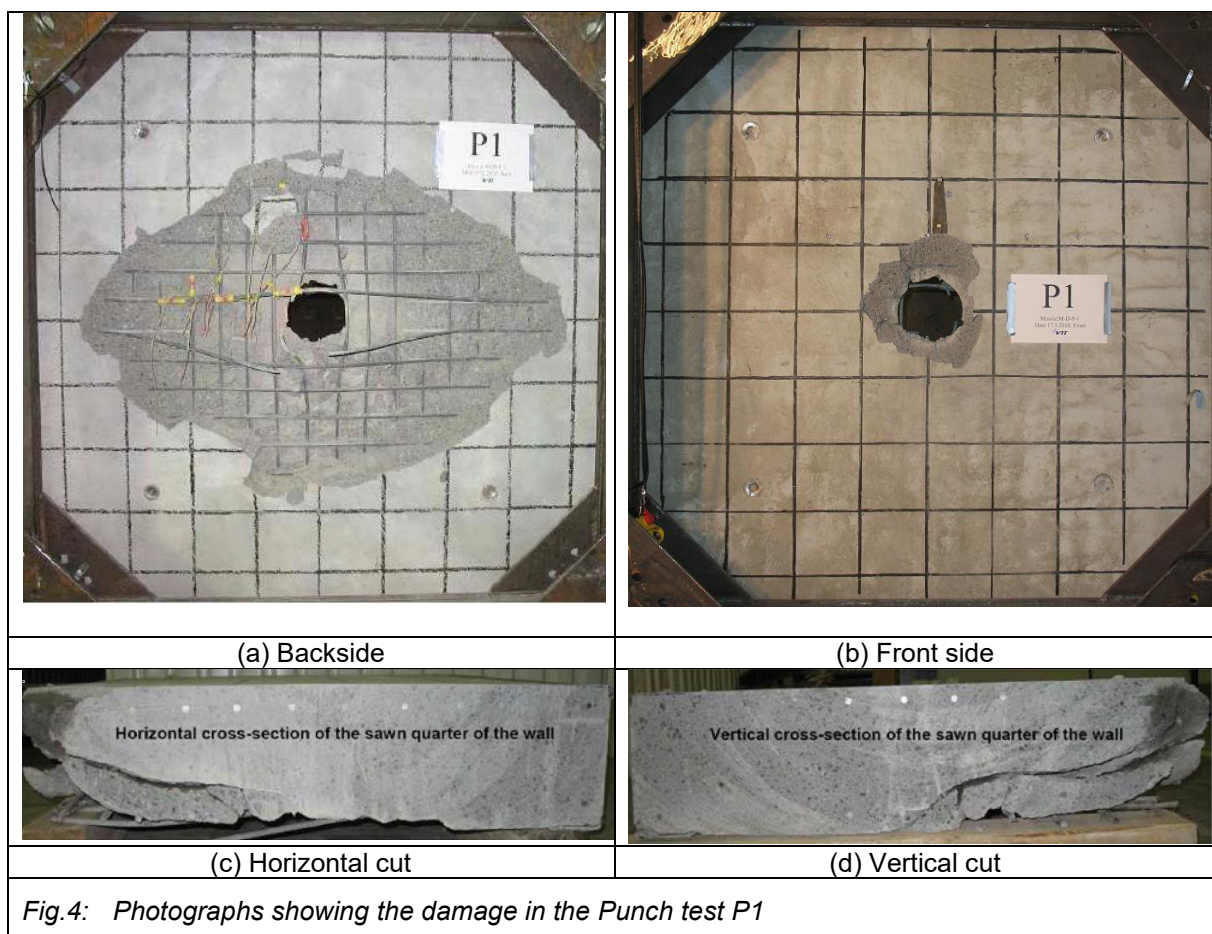


Fig.4: Photographs showing the damage in the Punch test P1

3 Finite Element (FE) Model

3.1 Hard Missile

Regarding the missile modeling in 2025, there are no significant changes to mention. A 3-D finite element model is developed for the whole missile (Figure 6). Solid elements **ELFORM** = -1 were used for modelling steel nose & pipe as well as **ELFORM** = 1 for the light-weight concrete filled inside the missile. The constitutive material model used to model the steel parts of the missile is ***MAT_PLASTIC_KINEMATIC** (see Table 2), while the constitutive model used to model the concrete filling is ***MAT_72R3**. Strain rate effect is not included since the strength of hard missile is not sensitive.

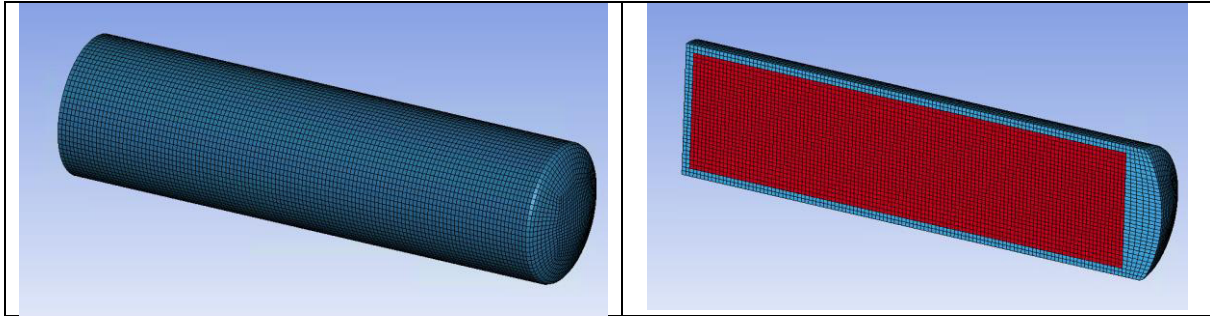


Fig.5: Finite Element model for Hard Punch Missile

Table 2: Steel Material parameters for Nose & Pipe Missile

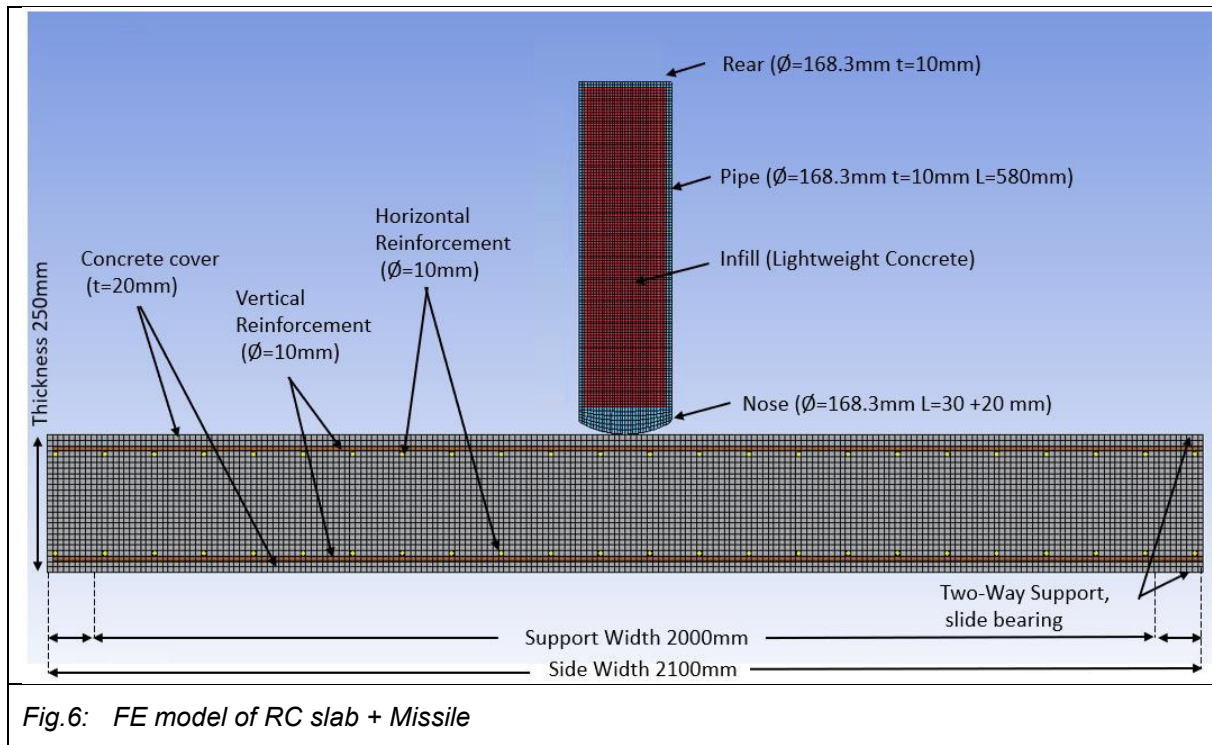
*MAT_PLASTIC_KINEMATIC							
\$#	mid	ro	e	pr	sigy	etan	beta
	1000127	.85000E-9	210000.0	0.3	355.0	1646.0	0.0
\$#	src	srp	fs	vp			
	0.0	0.0	0.0	0.0			

Table 3: Light-Weight Concrete parameters for Infill part

*MAT_CONCRETE_DAMAGE_REL3_TITLE								
concrete_filling_missile								
\$#	mid	ro	pr					
	1000051	.56900E-9	0.2					
\$#	ft	a0	a1	a2	b1	omega	alf	
	0.0	-5.0	0.0	0.0	0.0	0.0	0.0	
\$#	slambda	nout	edrop	rsize	ucf	lcrate	locwidth	npts
	0.0	0.0	0.0	0.03972	145.0	0	0.0	0.0
\$#	lambda1	lambda2	lambda3	lambda4	lambda5	lambda6	lambda7	lambda8
	0.0	0.0	0.0	0.0	0.0	0.0	0.0	0.0
\$#	lambda09	lambda10	lambda11	lambda12	lambda13	b3	a0y	aly
	0.0	0.0	0.0	0.0	0.0	0.0	0.0	0.0
\$#	eta1	eta2	eta3	eta4	eta5	eta6	eta7	eta8
	0.0	0.0	0.0	0.0	0.0	0.0	0.0	0.0
\$#	eta09	eta10	eta11	eta12	eta13	b2	a2f	a2y
	0.0	0.0	0.0	0.0	0.0	0.0	0.0	0.0

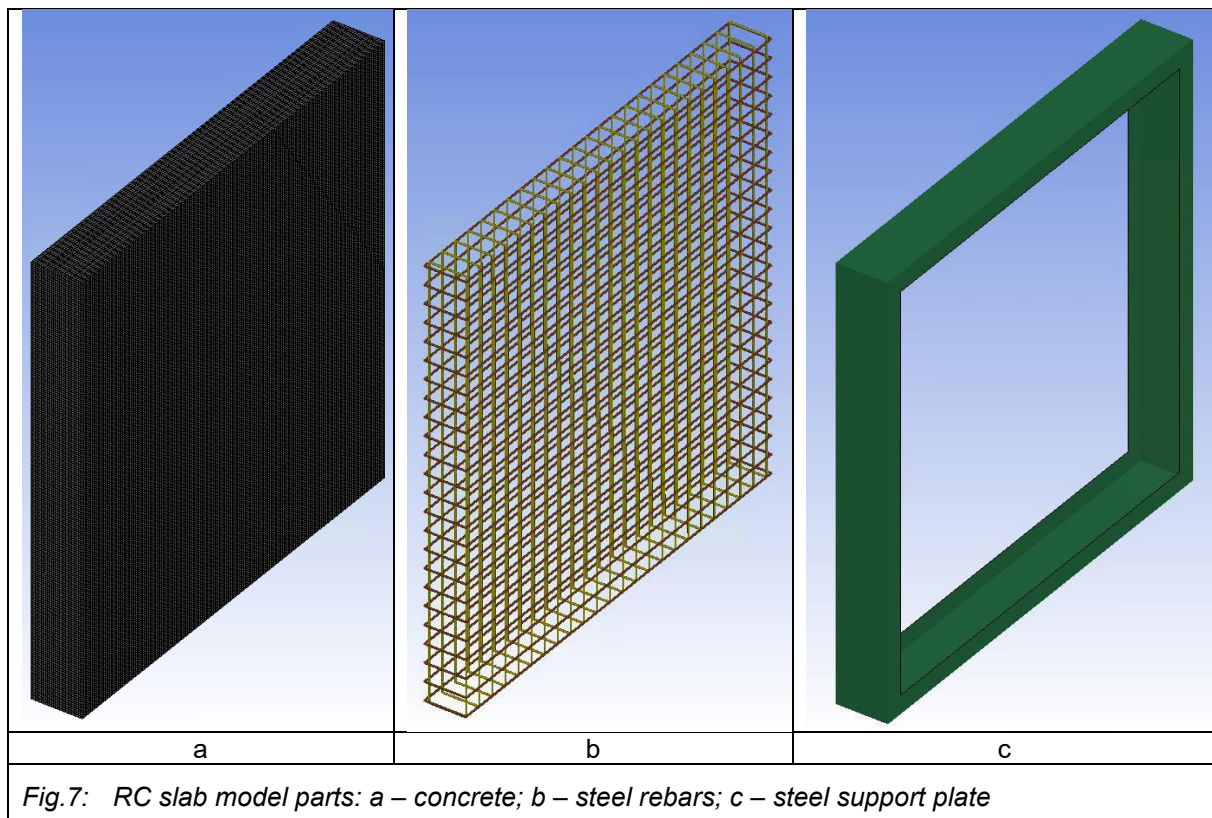
3.2 Reinforced Concrete (RC) Slab

As previously described for VTT test, the RC slab is composed of two uncoupled layers of steel rebar for reinforcement: There are no shear rebars or stirrups linking the two layers of reinforcement bars. A section view to describe the FE model is shown in figure 6.



The model mixes different types of elements (see Fig. 7)

- Concrete: Hexahedral solid elements **ELFORM** = 1 are used with Hourglass controls (**IHQ** = 3, **QH** = 0.01) to prevent unphysical & asymmetric damage accumulation in the material.
- Reinforcing rebars: Hughes-Liu beams with cross-section integration
- Steel Plate support: Belytschko-Tsay shell elements with three integration points and **IHQ** = 4, **QH** = 0.1 are used for Hourglass



*CONSTRAINED_BEAM_IN_SOLID card is used to embed reinforcement beams in concrete (no sliding permitted) with constrained equations and avoid merging nodes together. Additionally, the vertical and horizontal rebar beams are not merged. To ensure optimal coupling with the reinforcement bars, the concrete mesh size should equal the bar diameter and so, the mesh size was set to 10 mm.

To simplify the model, the support plate is merged with concrete edges and SPC Boundary conditions are put in place where the cylinders are directly in contact (see Fig.3).

All steel elements of the slab are modeled with *MAT_PIECEWISE_LINEAR_PLASTICITY (see Table 4 & fig- 9). According to IAEA recommendations, the strain-rate effects are accounted for using the Couper-Simonds model ($C = 40 \text{ s}^{-1}$, $p = 5$) in the case of experimental data absence [5]. The failure criterion is fixed to 12% of plastic strain.

Table 4: Reinforcement rebars Material parameters

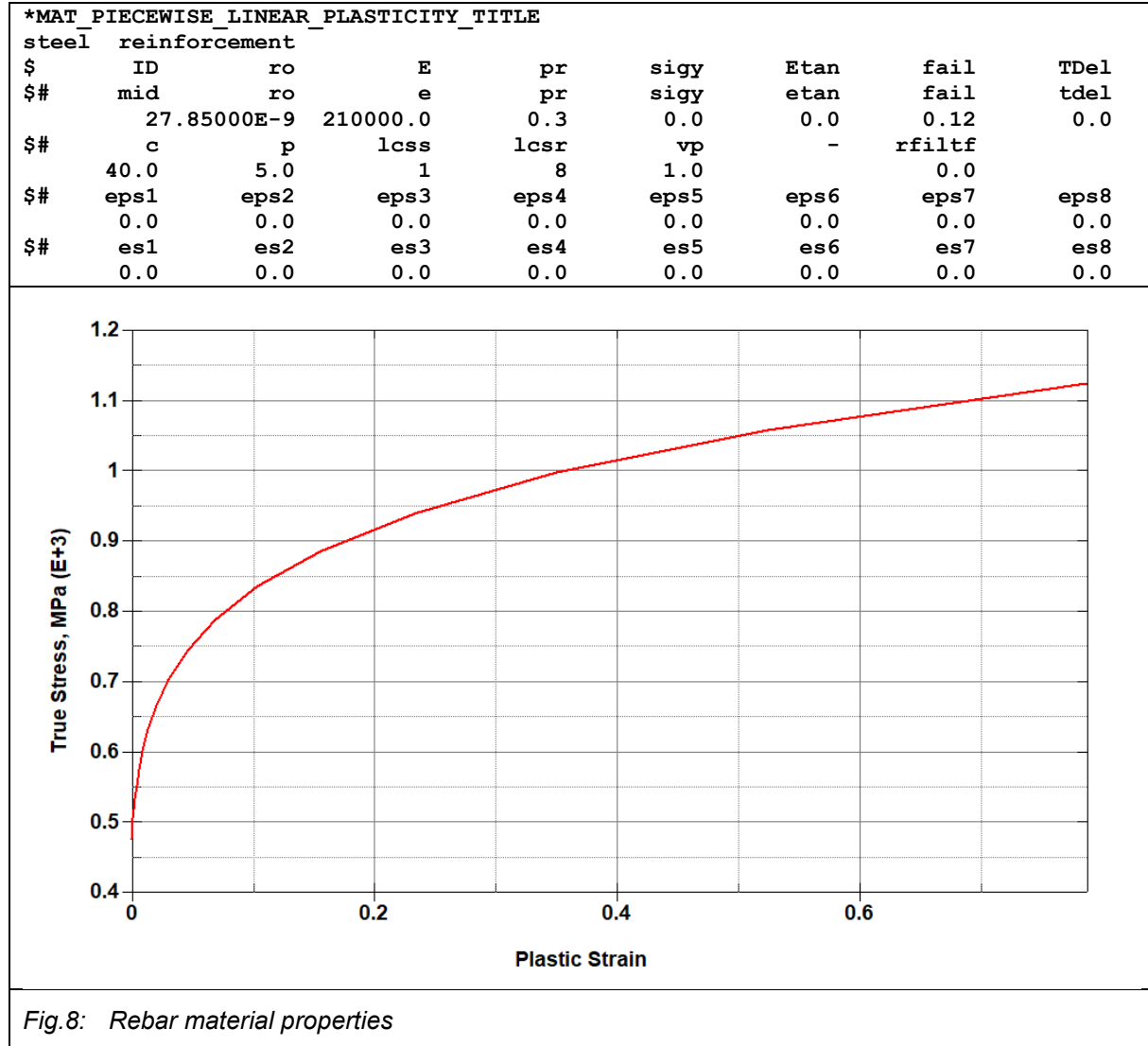


Fig.8: Rebar material properties

As mentioned in introduction, the benchmark IRIS_2010 is an exercise in OECD/NEA/CSNI framework [2]. This exercise concentrated on improving robustness assessment methodologies for structures impacted by missiles. As Phase I involved the blind prediction of the response of two missile impact tests, the concrete data provided below was the only one information (see table4)

Table 5: Concrete data provided for IRIS 2010

Material: reinforced concrete	
Concrete:	
Young modulus (secant value at $f_c/3$):	29053 MPa
Dynamic Poisson's ratio between	0.186 and 0.295
Concrete resistance in compression ⁽¹⁾ f_c :	37.2 MPa
Concrete resistance in traction f_t :	4.8 MPa

In this context, ***MAT_CSCM_CONCRETE** has been chosen with $F_c=37.2\text{MPa}$ including new calibration suggested by Yury Novozhilov [4] (see Table 6). This is a Continuous Surface Cap Model for concrete material [9]. With the updated calibration procedure found in 2022, all ***MAT_CSCM** model parameters (see Table 5) can be identified based on density, axial compressive strength, and fracture energy (which can be calculated based on the characteristic size of the aggregate). For this procedure's application, the aggregate's characteristic size is assumed to be 19 mm.

Table 6: Continuous Surface Cap Model parameters for concrete material

*MAT_CSCM_TITLE									
C37.2									
\$#	mid	ro	nplot	incre	irate	erode	recov	itretc	
	1000042.26100E-9		1	0.0	1	1.05	10.0	0	
\$#	pred								
	0.0								
\$#	g	k	alpha	theta	lamda	beta	nh	ch	
	11910.0	17290.0	10.10722	0.3356309	4.595342	0.0366455	0.0	0.0	
\$#	alpha1	theta1	lamda1	beta1	alpha2	theta2	lamda2	beta2	
	0.82	0.0	0.2407	0.0106624	0.76	0.0	0.26	0.0093868	
\$#	r	xd	w	d1	d2				
	2.129992	87.4694	0.0656	0.11000E-42	0.22500E-6				
\$#	b	gfc	d	gft	gfs	pwrc	pwrt	pmod	
	100.0	8.624187	0.1	0.0862419	0.0862419	5.0	1.0	0.0	
\$#	eta0c	nc	etaot	nt	overc	overt	srata	rep0w	
	1.19500E-4	0.786	0.89400E-5	0.48	24.96275	24.96275	1.0	1.0	

The finite element method (FEM) is a way to calculate how strong concrete structures are. It can be used to find the response of a structure when it is put under extreme pressure. But there is a problem: sometimes, a finite element gets really distorted. This can make the Jacobian determinant negative, which causes the volume and the element to stop working. Also, the finite element can't change the way the structure is built, so it doesn't solve issues with perforation. To deal with problems from distorted elements, the element erosion technique is often used. With this, the user chooses a failure criterion (for example, a strain limit or damage value), and then the technique removes the distorted elements. But the element erosion technique also has problems: it's dependent on the mesh size, damaged concrete isn't considered when interacting with other objects, and mass and momentum is lost. This leads to incorrect results and limits its use.

An alternative approach is to use the mesh-free method, which is well-suited to high deformation, large strain, and material fragmentation. The most popular mesh-free method is smooth particle hydrodynamics (SPH), which was developed for astrophysical problems and adopted for applied mechanical problems. One disadvantage of the SPH method compared to the finite element method (FEM) is its high computational cost but the interaction between crushed concrete in SPH and the reinforcement mesh is also currently impossible [8]. In our case, the solution is the DES approach [10]. The method introduced with ***DEFINE_ADAPTIVE_SOLID_TO_DES** (see fig.10) avoids loss of damaged concrete mass by considering the ultimate state of damaged concrete to be nothing more than sand (see Table 7) [7]. The criterium to switch SOLID to DES is defined when the concrete is fully damaged with an effective strain of 5% (**EROD** = 1.05). The contact with projectile is so maintained during the perforation with a classical contact. It is recommended to set **FS** = 0.6, **FD** = 0.4 and increase the penalty coefficients on the FE side by a factor of 60 [7]. ***DEFINE_DE_TO_BEAM_COUPLING** allows to interact the concrete sand with reinforcement bars with following suggested parameters: **FRICS=FRICD=0.45**, **DAMP** = 0.5, **BSORT** = 100[7] which allows realistic retention of concrete fragments inside the reinforcement cage.

Table 7: Parameters for DES discrete elements

*CONTROL_DISCRETE_ELEMENT								
\$#	ndamp	tdamp	fric	fricr	normk	sheark	cap	mxnsc
	0.5	0.5	0.57	0.1	0.01	0.0029	0	0

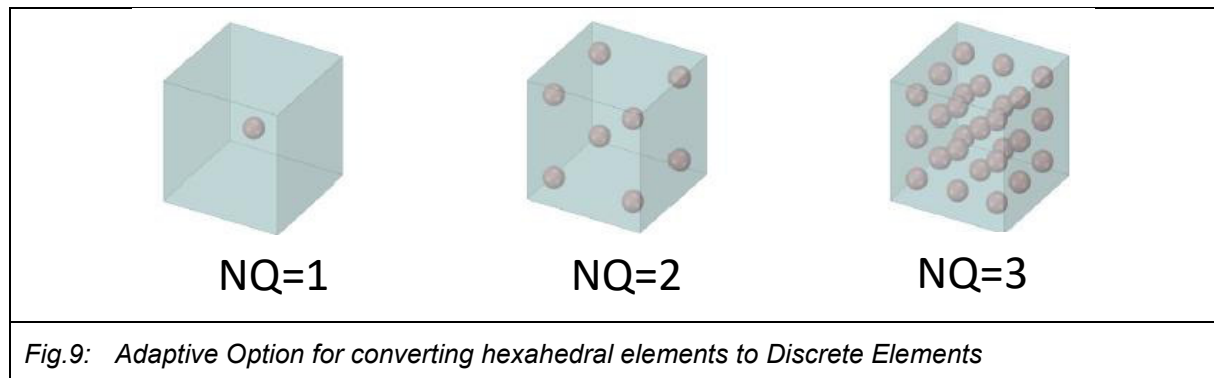


Fig.9: Adaptive Option for converting hexahedral elements to Discrete Elements

4 Simulation results

4.1 IRIS 2010

The revisited simulation revealed the complete perforation of the concrete wall with a residual velocity of 41.5m/s, a velocity within the experimental margin of error, with a minimum residual speed of 33.8 m/s and a maximum speed of 45.3 m/s (see table 1).

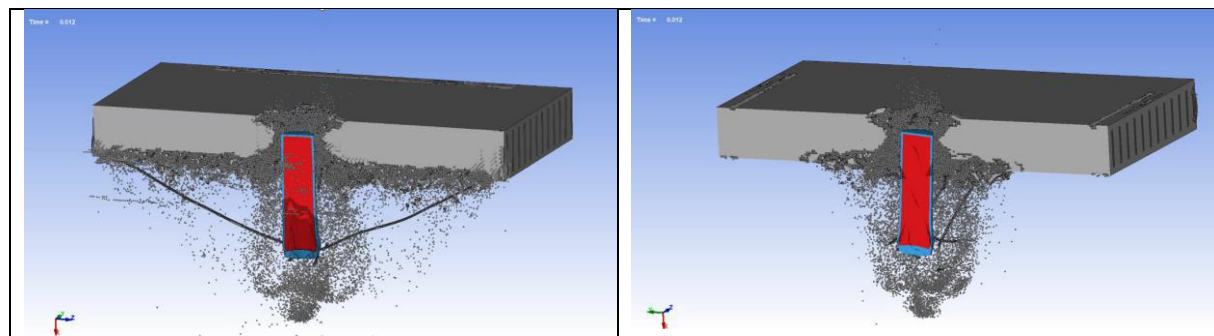


Fig.10: Missile perforation

In terms of Concrete slab damage, there are similarities with the tests, but the rear face seems to be the most damaged.

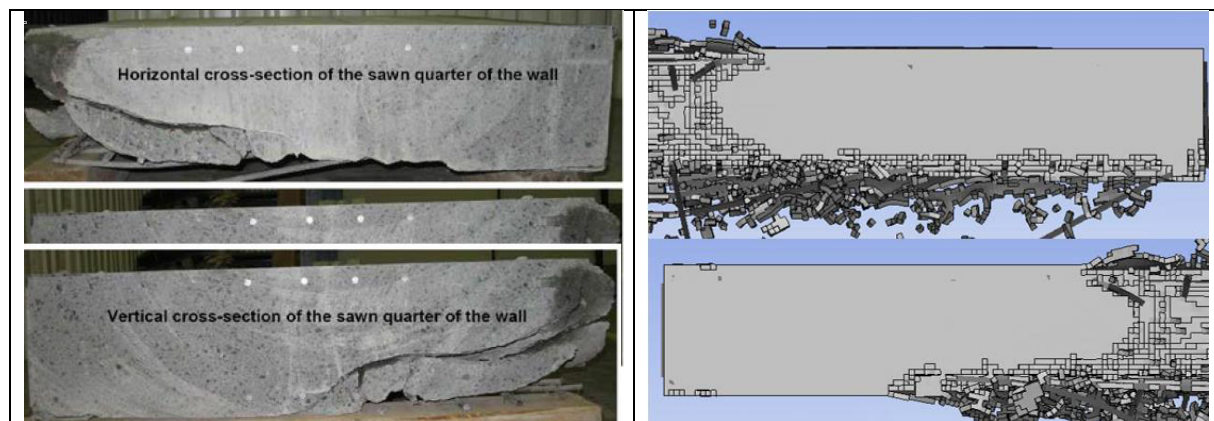


Fig.11: Comparison with a quarter slab

The second layer of reinforcement (near back face) plays a significant role in residual speed here: reinforcement bars slow down the missile as they gradually disengage from the concrete, like a delamination.

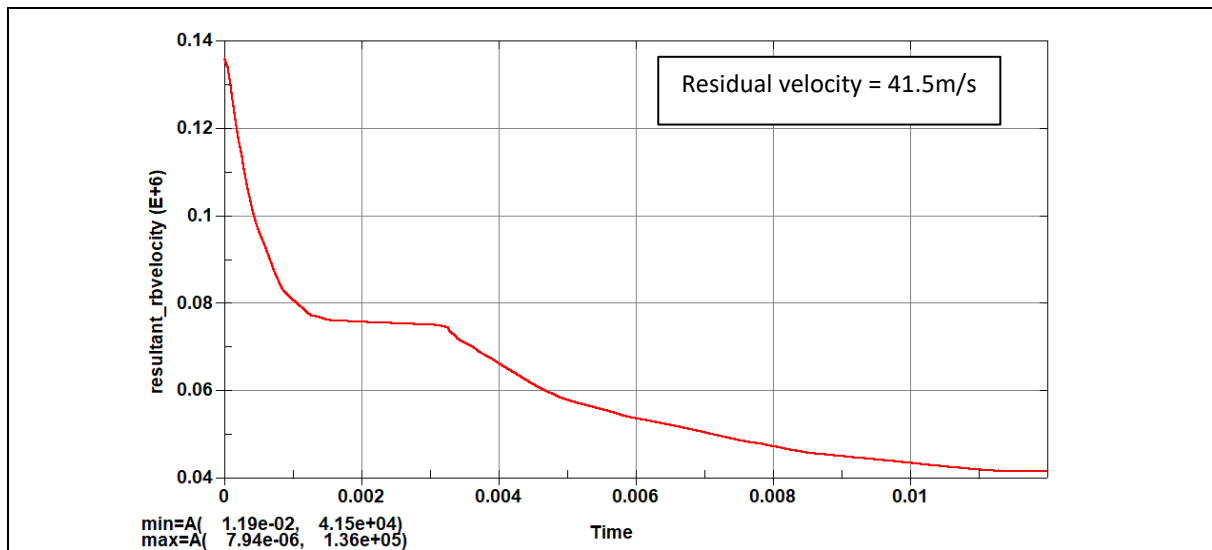


Fig.12: Missile velocity during the impact

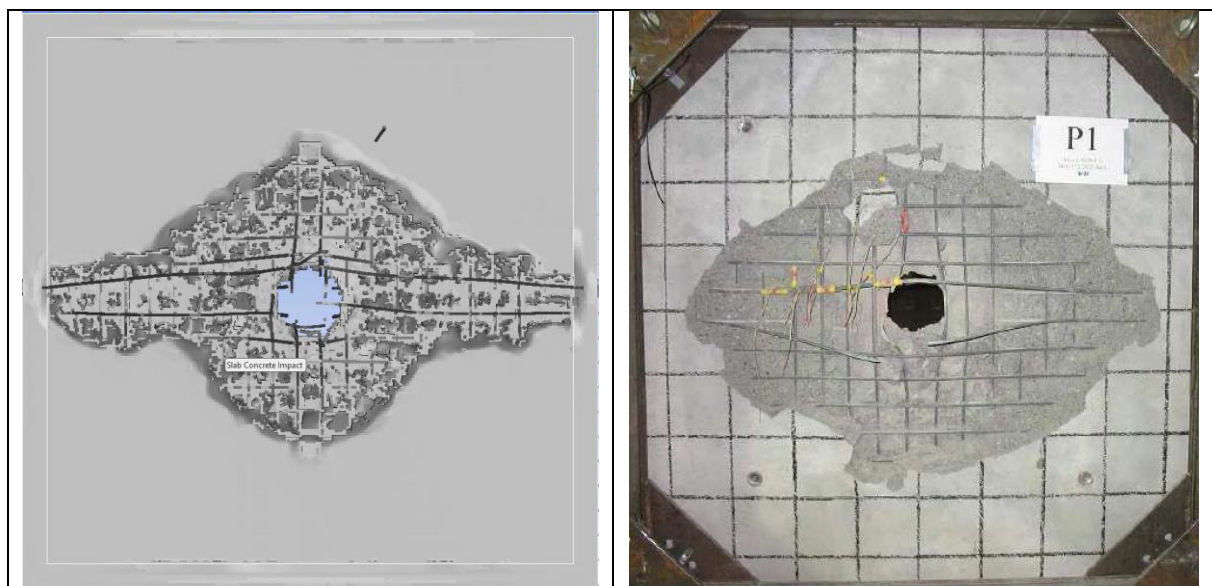


Fig.13: Back face of slab

The scabbled area on the back of the concrete slab runs along the entire length of the wall, mainly caused by 2 reinforcement bars which act as arresting wires as is the case on an aircraft carrier.

The front face is more damaged than in the test, with apparent reinforcement rebars (see fig 14).

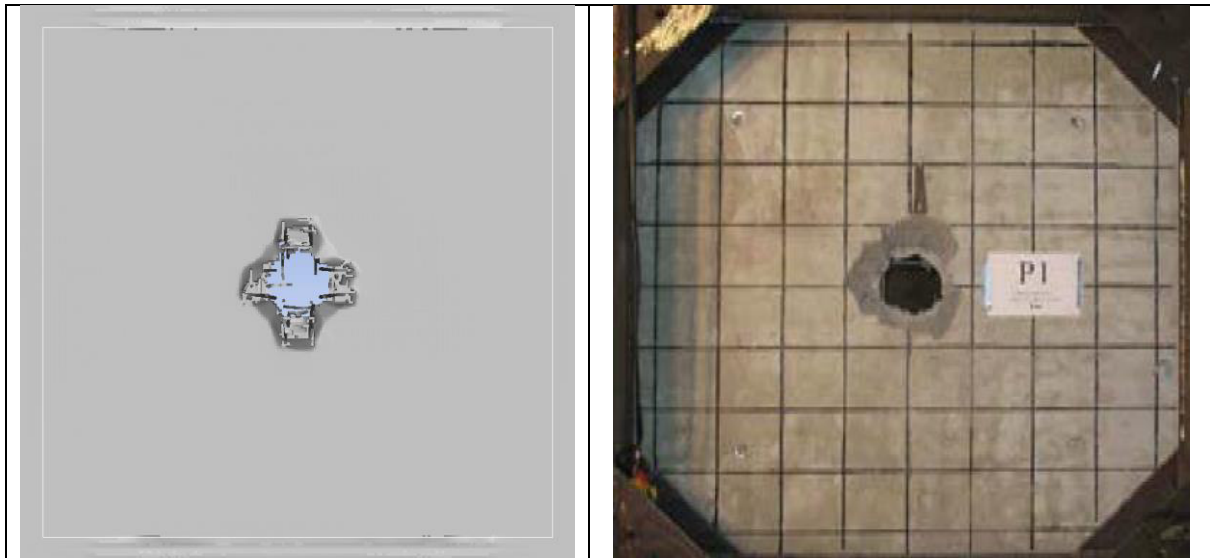


Fig.14: Front face of slab

4.2 IRIS 2012

The outcome of the first phase, completed in 2010, was not encouraging with regard to the results obtained by the different simulation teams [2]. The second phase was launched again in 2012 to improve the simulation results and bring them closer to the experimental results. Concrete data was provided from additional characterization tests based from cylinder concrete specimens [3] (see table 8).

Table 8: Concrete Property for Model Calibration

	Unconfined	Confined
Density, ρ	22610 kg/m ³	22610 kg/m ³
Compressive Strength, σ_c	69.0 MPa	66.93 MPa
Young's Modulus, E	29663 MPa	29670 MPa
Poisson Ratio, ν	0.22	0.223
Aggregate Size, A	19.0 mm	19.0 mm

Simulation results with the modified concrete are little bit surprising because they led to a slightly higher residual velocity (42.1 m/s) (see fig. 15) with harder concrete. The residual velocity results obtained are within the experimental margin of error and are fairly close to those obtained with the 2010 concrete data.

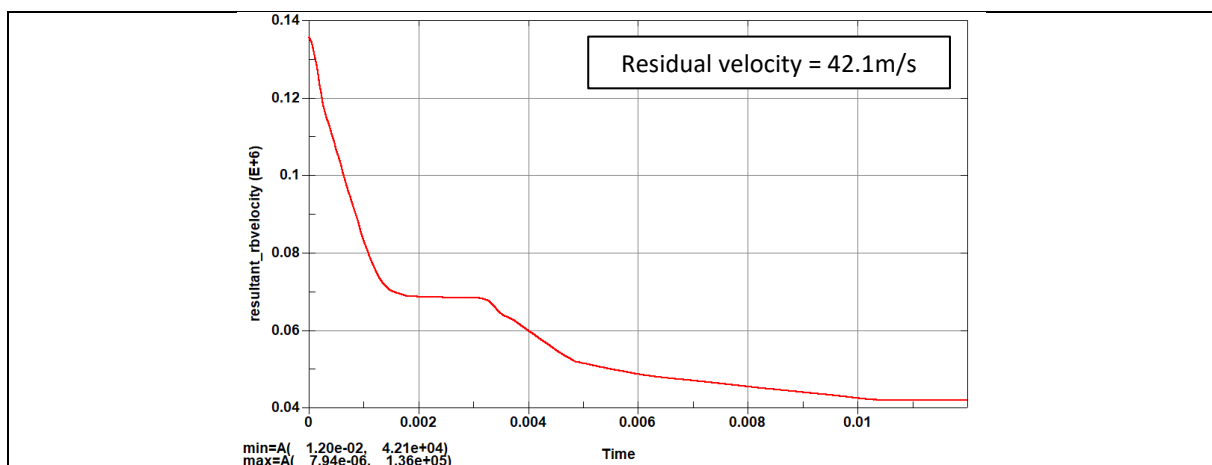


Fig.15: Missile velocity during the impact

What can we say about these results? The comparison of the velocity curves shows two key points: the first is the effect of concrete stiffness, and the second is the influence of the reinforcement layer on the back face of the concrete slab (see fig 16). During the first 5 ms, the missile slows down considerably as it impacts the stiffest concrete but after 5ms, the missile sufficiently perforated the concrete to come into contact with the back layer of rebars: the only final resistance to the missile are 2 reinforcement rebars in each case (see fig.17)

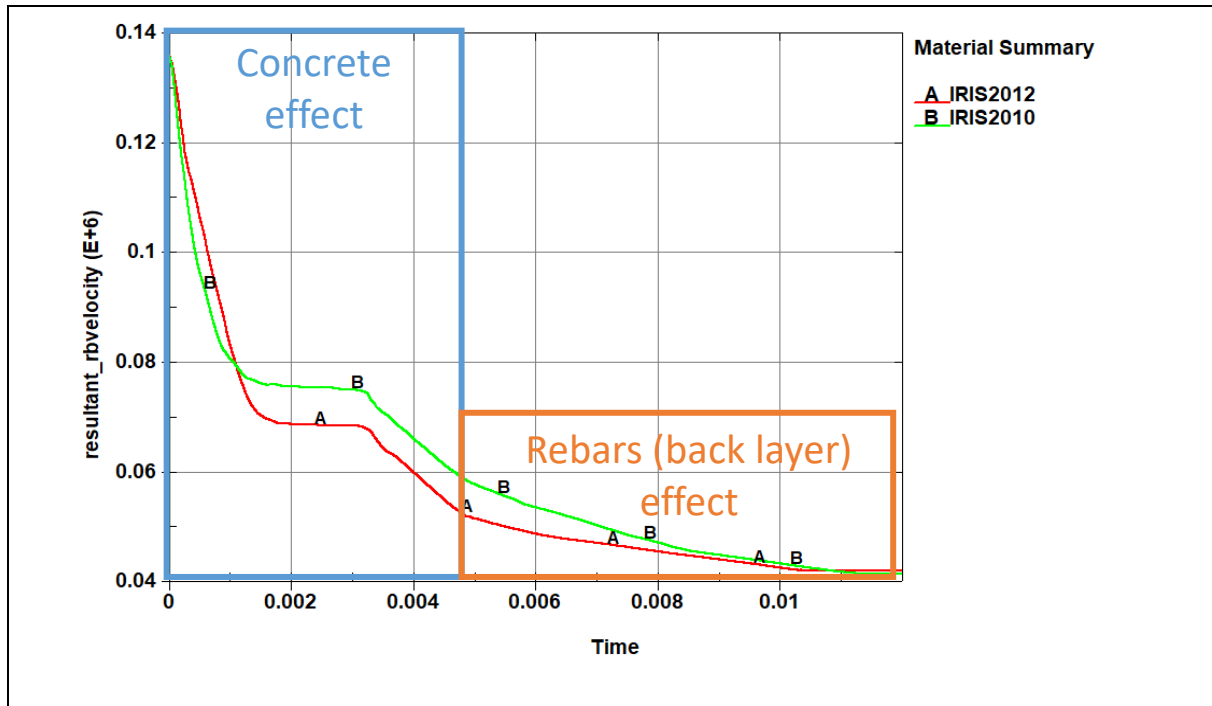


Fig.16: Comparison of missile velocity between 2010 & 2012 models

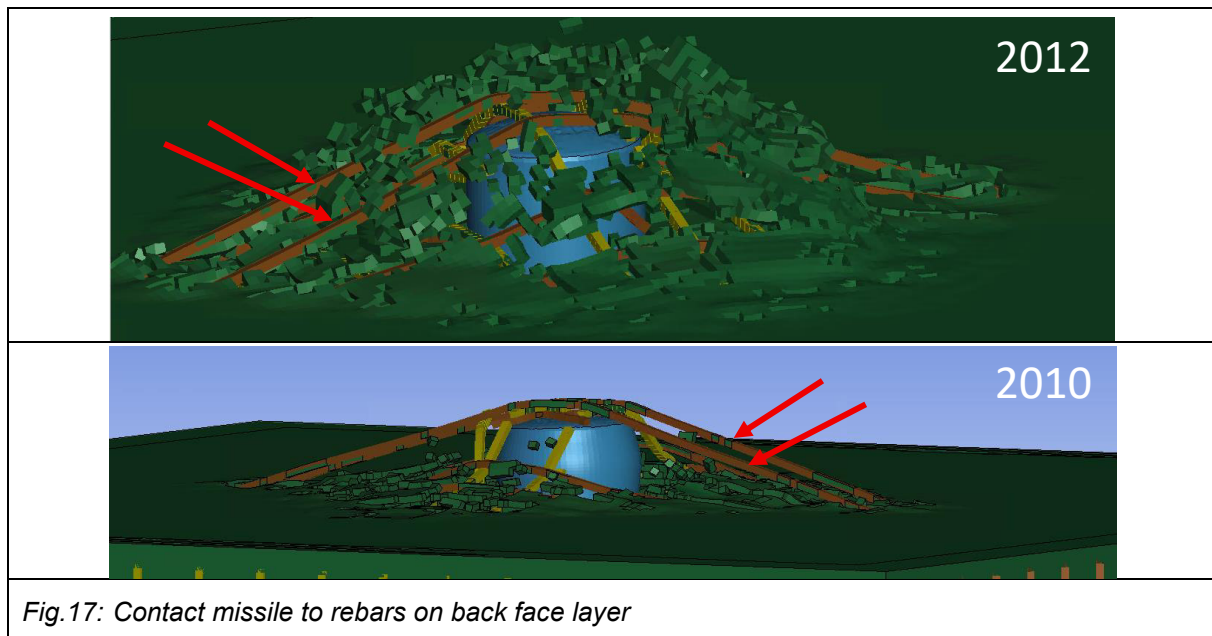


Fig.17: Contact missile to rebars on back face layer

After 5 ms, the velocity profile no longer has the same offset, and what differs between these 2 results is the timeline of rebar failure: With the 2012 model, one of the two reinforcement rebars breaks sooner

than with the 2010 model and so the velocity decreases fast because 2 rebars still remain in contact for the 2010 model (see fig 18 & 19).



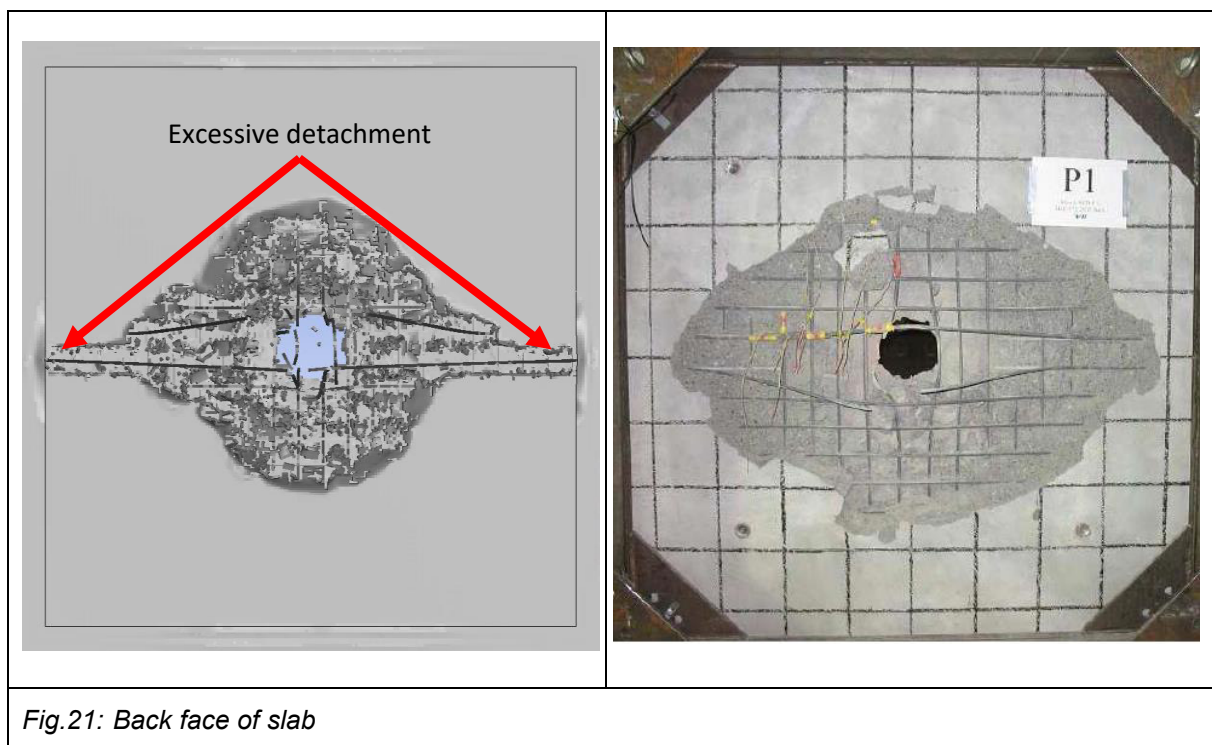
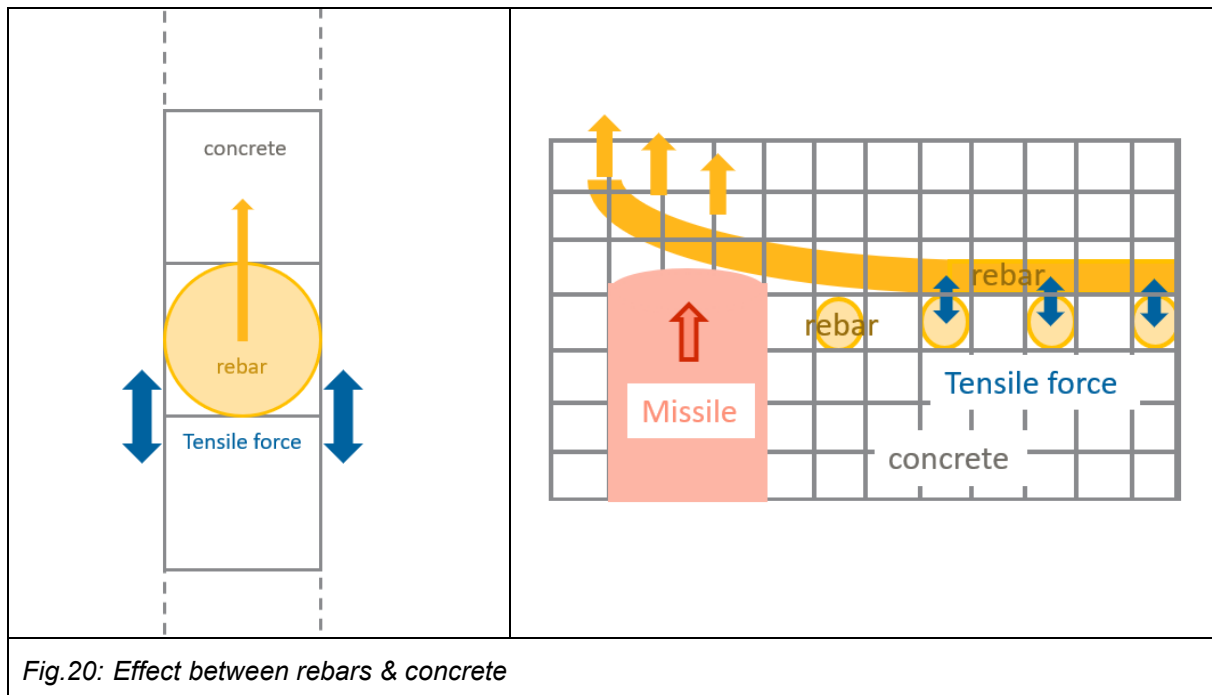
Fig.18: $T=6.5\text{ms}$ Only one rebar remains in contact with missile for 2012 model



Fig.19: $T=10.5\text{ms}$ no rebar to retain the missile for 2012 model

Although the damaged area is smaller (less than 1.05% effective strain), there is excessive bar detachment, indicating weak bar anchoring in the concrete or missing simulation elements. The scabbing on the back of the slab is slightly different compared to the real test. Some of the horizontal rebar is excessively detached from the concrete along almost its entire length (see fig 21).

This problem may be related to the way the reinforcement bars are coupled with the concrete. When the missile pushes on the reinforcement, the coupling connections directly stress the solid elements of the surrounding concrete because they are kinematically connected to the reinforcement. The concrete elements located directly beneath the reinforcement are so under tension (see Fig. 20) and Gradually, these elements accumulate damage until they reach their failure point, causing decoupling like delamination.



Possibly, by forcing the reinforcing bars to remain anchored, the residual velocity of the missile could be reduced while ensuring a deformation surface closer to the tests. This will be the subject of the next stage of this report, which will consist of studying the influence of some parameters.

4.3 Parameters influence

4.3.1 binding wire for reinforcement rebars

Unlike in the simulation, in real conditions, the vertical and horizontal rebar is linked together with steel wire (see Fig. 22). Naturally, these links provide additional stiffness and probably prevent excessive detachment of the rebar from the concrete. The rebar interacts as if it were a real net.



Fig.22: Real binding wire for reinforcement rebars

To determine the influence of such behavior, beams with a small cross-section were connected at each intersection of the vertical and horizontal reinforcement layers (see Fig 23)

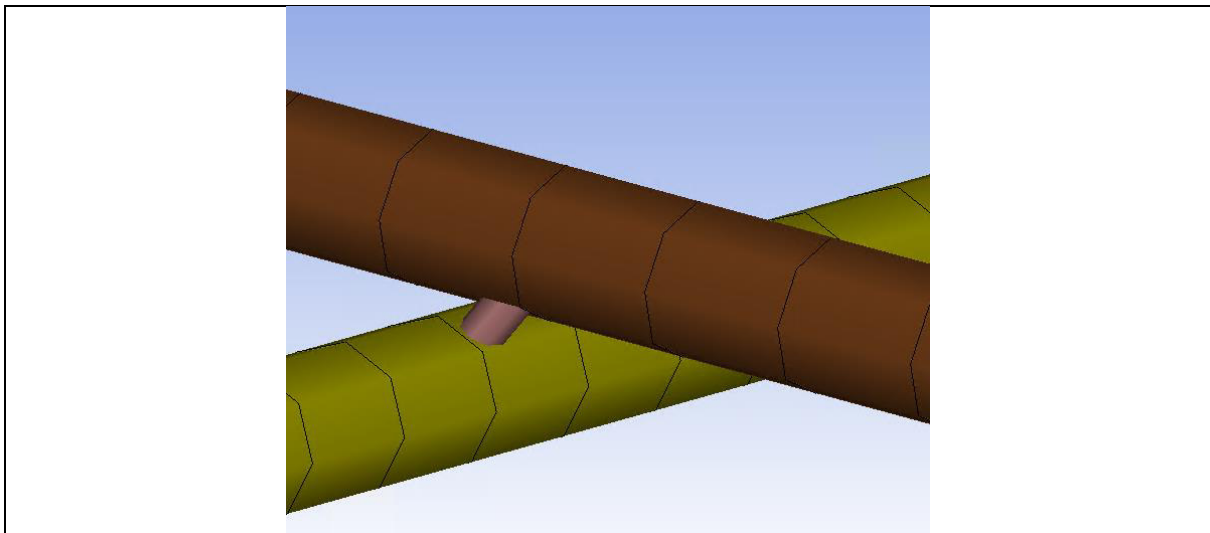


Fig.23: Binding wire in simulation

The chosen diameter is 3 mm, and the material is similar to rebar material, but without the effects of strain rates.

This modification slowed the missile down slightly, but the most significant aspect is the deformation caused to the rear face of the concrete panel. In fact, the spalling surface is now more precise (see Fig24.)

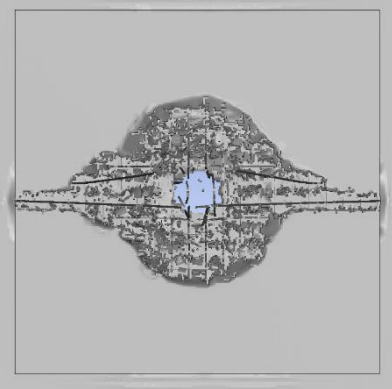
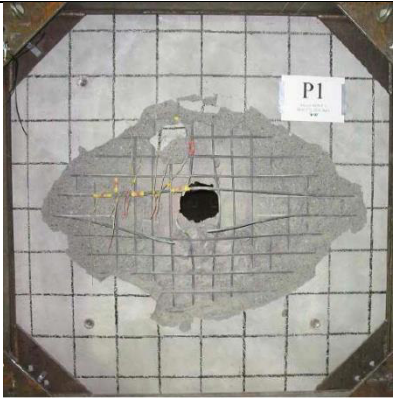

		
IRIS 2012 model	VTT Test	IRIS 2012 model modified with binding wire

Fig.24: Comparison of deformed rear concrete panel

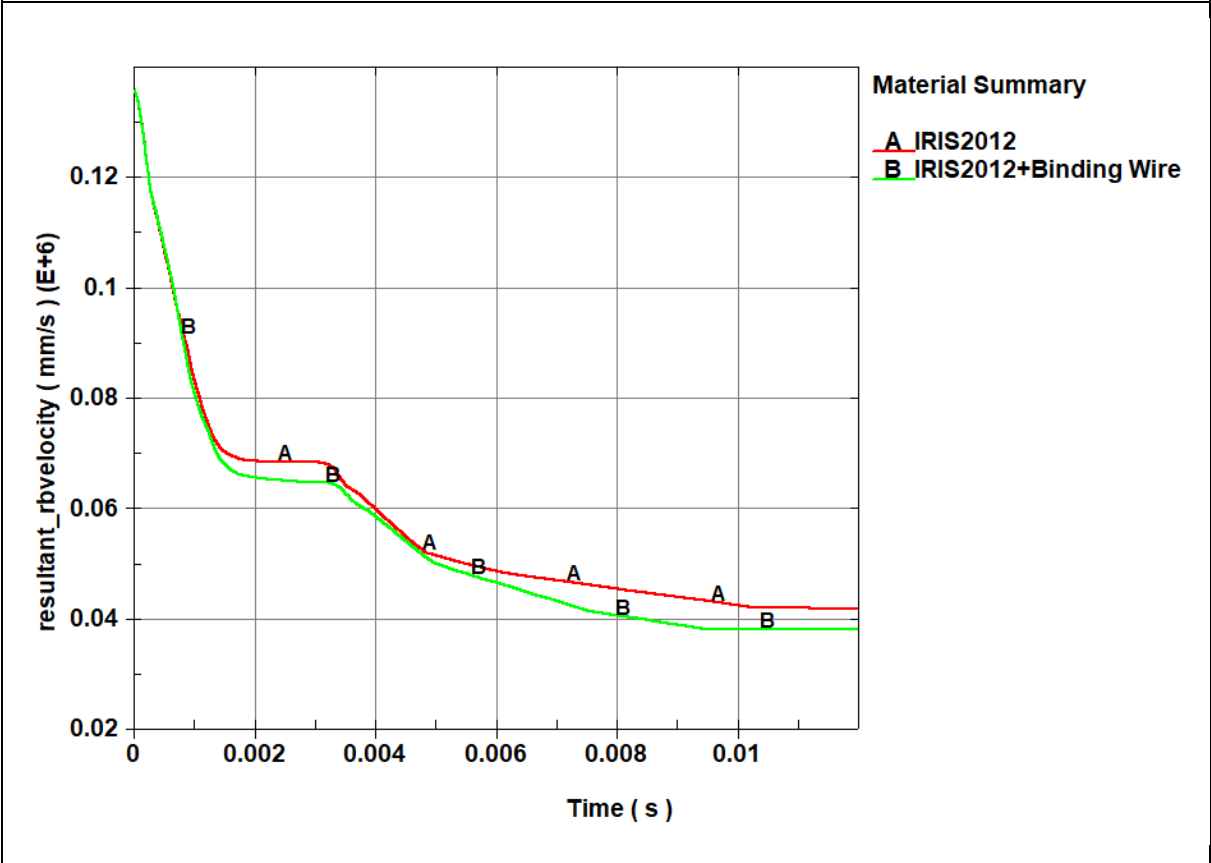


Fig.25: Comparison between model with & without bending wire

Figure 25 shows a residual velocity of missile below 40m/s with 38.2m/s. This model once again demonstrates significant and sensitive results (see table 1) according to reinforcement behavior which could explain the residual velocity gaps obtained during testing. As a reminder, the difference between the minimum and maximum values of test velocity is ~12 m/s. It is possible that the simulation may highlight this instability issue and why it was very difficult to predict the results in blind test conditions.

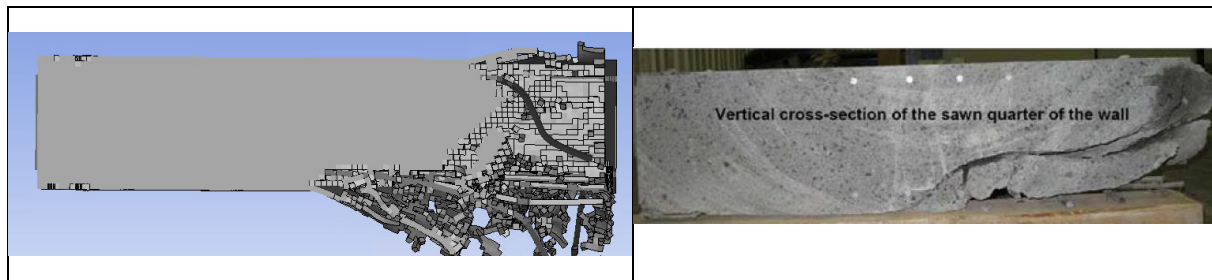


Fig.26: quarter of slab

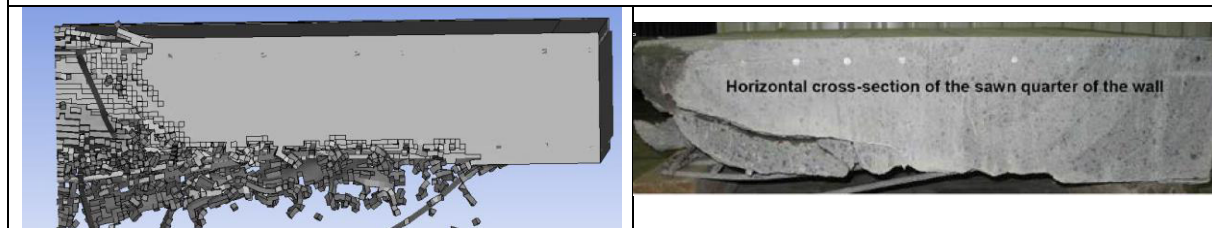


Fig.27: quarter of slab

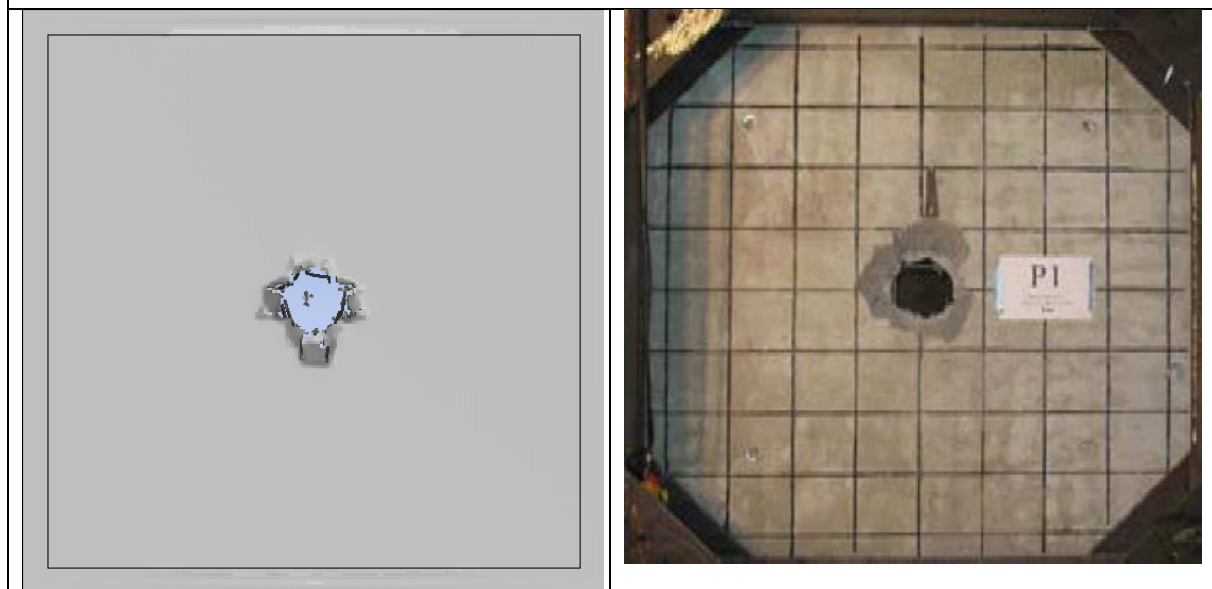
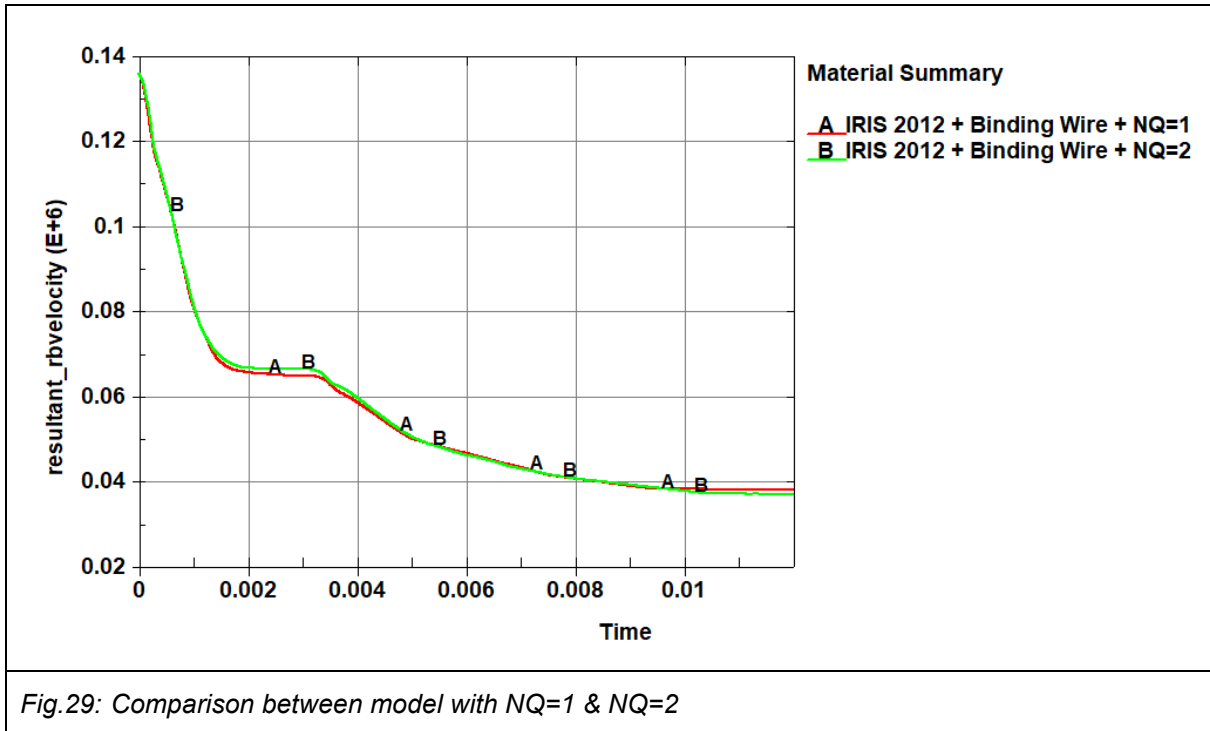


Fig.28: Front face of slab

4.3.1 number of DES generated by element

As the concrete material model is previously configured with the `*DEFINE_ADAPTIVE_SOLID_TO_DES` keycard (see fig.10) to replace the eroded element with one DES particle when the principal strain threshold of 5% is reached. Since the solver can create one or more discrete rigid sphere elements for each eroded element (see fig. 9), let's try `NQ=2`. This means that four particles will be generated for each solid element that is eroded. This will make it easier to evaluate the dynamic behavior of a larger amount of debris and any friction that is caused.



As shown in the figure 29, the parameter does not significantly impact the results. However, replacing a solid element with four particles ($NQ=2$) takes three to four times longer than replacing it with one particle ($NQ=1$).

4.4 Smoothed Particle Galerkin Method

The SPG method is a new, mesh-free method developed to model semi-brittle and ductile material failure[11]. SPG introduces a bond-based failure criterion for materials to reproduce strong discontinuities in the displacement field (without eroding damaged material) while conserving mass, momentum, and energy. So, the SPG method is well suited for modeling material failure such as Concrete in high velocity impact.

Converting the Model from FE to SPG requires a few steps. SPG exactly uses same input as FEM, except the section definition **SECTION_SOLID_SPG** with the formulation **elform=47** to activate SPG approximation, and of course, the **ADAPTIVE_SOLID_TO_DES** feature is removed. For high velocity deformations such as Impact penetration, **KERNEL=2**, normalized support sizes **DX,DY,DZ = 1.5** and **SMSTEP=30**, **ITB=2** are recommended. **IDAM=1** is chosen to simulate concrete damage behavior with **FS=0.99**. As for the **STRETCH** parameter, it was set to 1.005 instead of the recommended default value of 1.01 after a calibration (see table 9). Same material models as used FEM except **ERODE=0** for **MAT_CSCM**

Table 9: Section Properties for Solid SPG

*SECTION_SOLID_SPG									
\$#	secid	elform	aet	-	-	-	cohoff	gaskett	
	1	47	0				0.0	0.0	
\$#	dx	dy	dz	ispline	kernel	-	smstep	msc	
	1.5	1.5	1.5	0	2		30	0.0	
\$#	idam	fs	stretch	itb	msfac	isc	boxid	pdamp	
	1	0.99	1.005	2	0.0	0.0	0.0	0.0	

Of course, to reduce computational cost, only a small portion of concrete slab could have been approximated by the SPG formulation, especially around the impact area while the rest of concrete slab would be done with FEM but It was not the case here. The mesh size is identical with the previous models with FEM method.

The coupling with rebars needs to be replaced with SPG formulation in using ***CONSTRAINED_IMMERSED_IN_SPG** and to allow itself contact between particles, **CONTACT_SPG** needs to be added too.

The SPG method produces some interesting results (see figures 30 and 31): the residual velocity of the missile is close to the results previously obtained using the DES+FEM method, at 42.8 m/s. At first glance, the damaged back face of the slab also appears quite similar to the test. The comparison with previous curves once again demonstrates the influence of the back rebars layer and, above all, the method of coupling the rebar and concrete together (see Fig. 34). As previously, the last rebar impact appears to be the point of divergence, and this also seems to be the case in the tests.

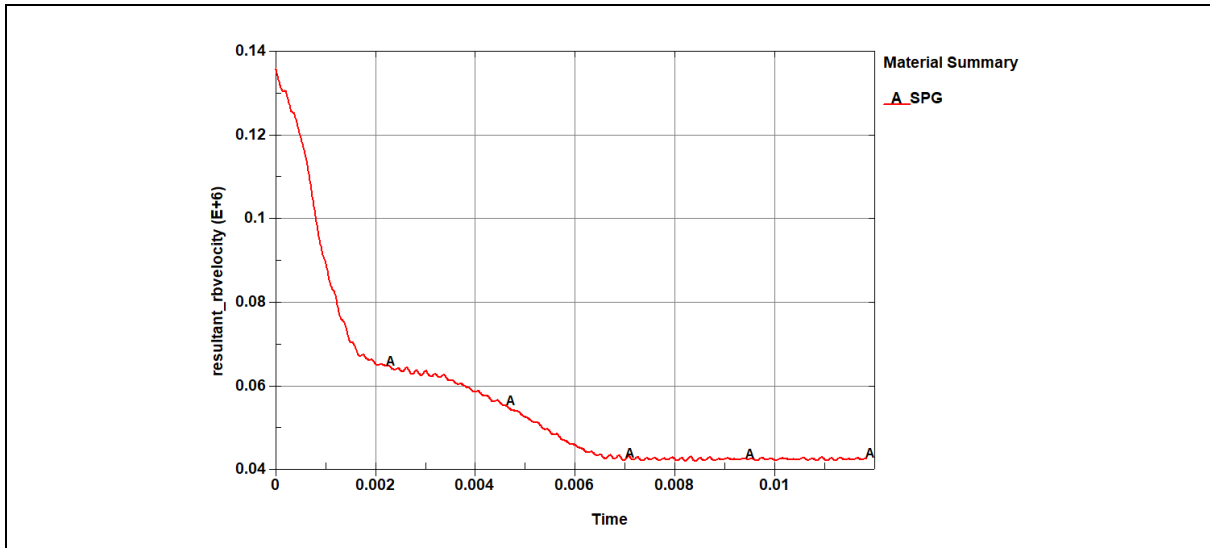


Fig.30: Missile velocity with SPG concrete slab Model

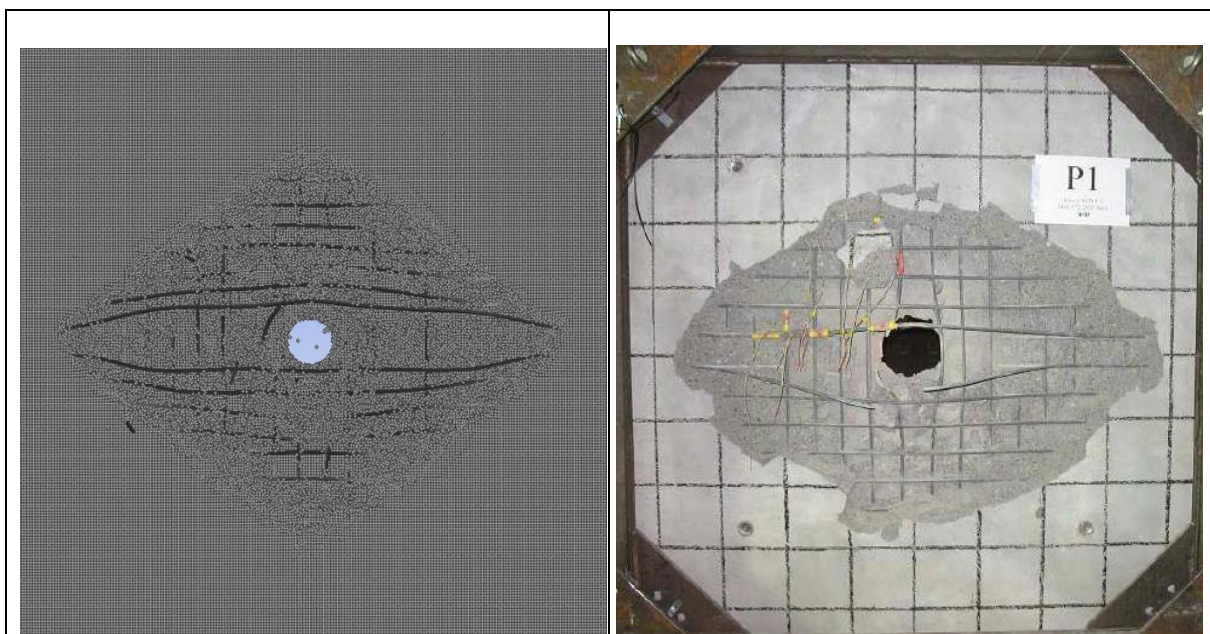


Fig.31: Back face of slab

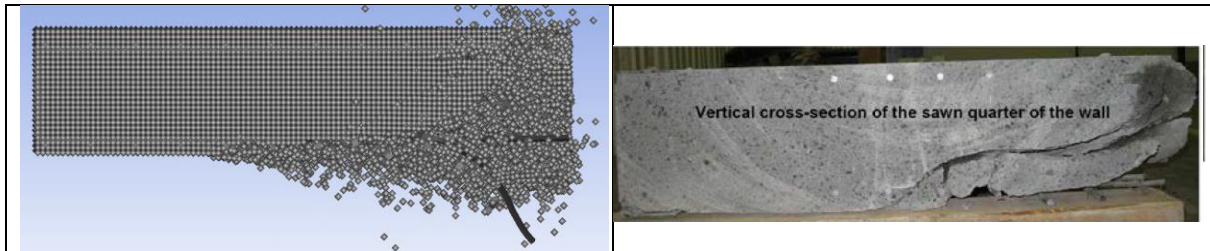


Fig.32: quarter of slab

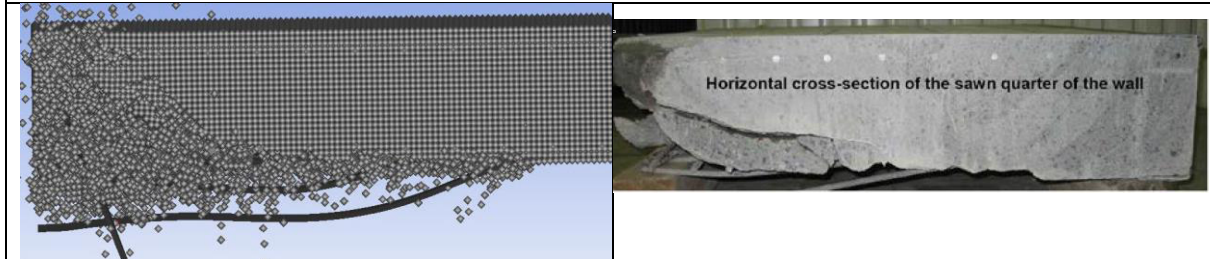


Fig.33: quarter of slab

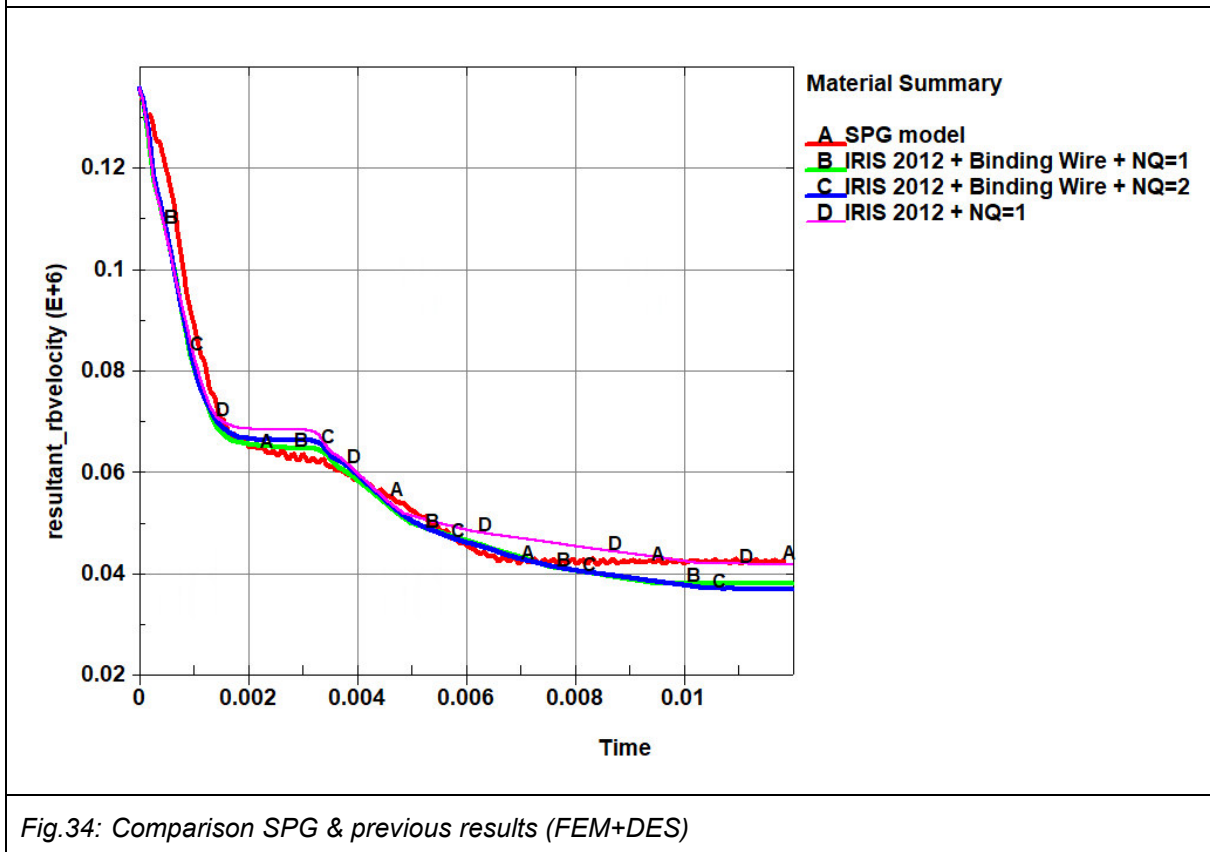


Fig.34: Comparison SPG & previous results (FEM+DES)

In any case, this particle-based method seems promising, with a computation time that is 1.5 times faster than the FEM+DES method. However, further research is needed to use this method and address the issues of perforation. SPG development is still in progress: an executable development version is still required to run on multiple cores, otherwise we encounter problems with the decomposition of the reinforcement bars and their coupling with the concrete.

Post-processing also needs improvement because the display requires converting solid elements into particles, which makes it both slow and complicated with current versions of LS-Prepost.

5 Summary

The new features and methods associated with more accurate calibration of CSCM concrete material enable an interesting step forward: the results tend to be closer to those obtained in tests in 2010. Indeed, the new method of replacing damaged and significantly deformed concrete elements with DES particles is an interesting approach for simulating complex concrete behavior, especially when the concrete is severely damaged. Nevertheless, achieving perfect predictability remains challenging, as demonstrated by the IRIS Punch example. While obtaining the residual velocity is one thing, faithfully reproducing the entire perforation phase is another. To achieve this, it is necessary to ensure reproducibility in real tests and to have sufficient output data with which to check the accuracy of the simulation. This adaptive method, which introduces a particle method, seems very promising, as does the SPG approach, since both ensure coupling between the particles and the reinforcement, and above all, both significantly improve the preservation of mass and momentum balance.

6 Literature

- [1] Ari Vepsä, Arja Saarenheimo, Francois Tarallo, Jean-Mathieu Rambach, Nebosja Orbovic, "Impact Tests for IRIS_2010 Benchmark Exercise, (2012), <https://doi.org/10.20965/jdr.2012.p0619>
- [2] NEA (2012), Improving Robustness Assessment Methodologies for Structures Impacted by Missiles (IRIS_2010): Final Report, OECD Publishing, Paris, <https://www.oecd-neo.org/upload/docs/application/pdf/2021-03/csni-r2011-8.pdf>
- [3] NEA (2014), Improving Robustness Assessment Methodologies for Structures Impacted by Missiles (IRIS_2012): Final Report, OECD Publishing, Paris, <https://oecd-neo.org/upload/docs/application/pdf/2021-02/csni-r2014-5.pdf>
- [4] Novozhilov, Y., et al., "Precise Calibration of the Continuous Surface Cap Model for Concrete," Simulation. Buildings, 12(5), 2022, <https://doi.org/10.3390/buildings12050636>
- [5] IAEA, Safety Reports Series No. 87: Safety Aspects of Nuclear Power Plants in Human Induced External Events: General Considerations. 2017, https://www-pub.iaea.org/MTCD/publications/PDF/PUB1769_web.pdf
- [6] Novozhilov, Y., et al., "Aircraft NPP Impact Simulation Methodology, " 16-Th International LS-DYNA Conference, 2020. <https://www.dynalook.com/conferences/16th-international-ls-dyna-conference/simulation-t9-2/t9-2-e-simulation-096.pdf/view>
- [7] Karajan, N., et al., "Particles as Discrete Elements in LS-DYNA: Interaction with themselves as well as Deformable or Rigid Structures," 11-th LS-DYNA Forum, Ulm, 2012, <https://www.dynalook.com/conferences/9th-european-ls-dyna-conference/interactionpossibilities-of-bonded-and-loose-particles-in-ls-dyna-r>
- [8] Dmitriev, A., et al., "Simulation of Concrete Plate Perforation by Coupled Finite Element and Smooth Particle Hydrodynamics Methods," Construction of Unique Buildings and Structures, 92(9207) 2020, <https://doi.org/10.18720/CUBS.92.7>
- [9] Murray, Y. D., et al., "Evaluation of LS-DYNA Concrete Material Model 159. In Federal Highway Administration", (2007), <https://www.fhwa.dot.gov/publications/research/infrastructure/structures/05063/05063.pdf>
- [10] Novozhilov Y " Adaptive FEM-DEM simulation of a soft projectile impact on a reinforced concrete slab (2024), https://www.dynalook.com/conferences/17th-international-ls-dyna-conference-2024/blast-impact-dynamics/novozhilov_cadfem.pdf
- [11] Y. Wu, C.T. Wu, Wei Hu, "parametric and Convergence Studies of the Smoothed Particle Galerkin (SPG) Method in Semi-brittle and Ductile Material Failure Analyses", (2018) <https://www.dynalook.com/conferences/15th-international-ls-dyna-conference/spg/parametric-and-convergence-studies-of-the-smoothed-particle-galerkin-spg-method-in-semi-brittle-and-ductile-material-failure-analyses>
- [12] John L. Bignell, Jonathan S. Rath, Syed A. Ali, and Richard F. Rivera-Lugo, " numerical simulation of a hard and a soft missile impact into a steel reinforced concrete target: overview of work performed by snl for the us nrc in support of the iris 2012 exercise", (2013), <https://www.osti.gov/servlets/purl/1299044>
- [13] Amirmohammad Samadzad, Matthew J. Whelan, " Effect of Hourglass Control on LS-DYNA Concrete Constitutive Models in Low Velocity Impact Simulations" , 2024

https://www.dynalook.com/conferences/17th-international-ls-dyna-conference-2024/blast-impact-dynamics/samadzad_university-of-north-carolina.pdf